Layer-by-Layer Hybrid Films Incorporating WO_3, TiO_2, and Chitosan

Fritz Huguenin,*,† Valtencir Zucolotto,‡ Antonio J. F. Carvalho,‡ Ernesto R. Gonzalez,§ and Osvaldo N. Oliveira, Jr.‡

Departamento de Química, Faculdade de Filosofia, Ciências e Letras de Ribeirão Preto—Universidade de São Paulo, 14040-901 Ribeirão Preto (SP), Brazil, Instituto de Física de São Carlos—Universidade de São Paulo, CP 369, 13560-970 São Carlos (SP), Brazil, and Instituto de Química de São Carlos—Universidade de São Paulo, 13560-970 São Carlos (SP), Brazil

Received May 25, 2005. Revised Manuscript Received October 25, 2005

Layer-by-layer (LbL) films from WO_3, TiO_2, and chitosan have been produced, in which the ability of complexation of chitosan with transition metal oxides was exploited. The electrochemical and chromogenic properties of LbL films of (chitosan/WO_3)$_4$/TiO_2 and (chitosan/WO_3/chitosan/TiO_2)$_4$ have been examined and compared to those of (chitosan/WO_3)$_4$. More specifically, we employed the quadratic logistic equation (QLE) to estimate the number of electrochemically active sites (K) and the molar absorption coefficient (ϵ) of WO_3 in LbL films, by fitting the absorbance changes (ΔA) resulting from the electron transfer from W(V) to W(VI) sites. The number of electrochemical active sites for 4-bilayer LbL films of chitosan/WO_3 before and after deposition of TiO_2 was ca. 15.5×10^{-9} mol cm^{-2} and 10.7×10^{-9} mol cm^{-2}, respectively. The incorporation of TiO_2 in the LbL films led to a larger absorption coefficient and electrochromic efficiency. The differences in the molar absorption coefficient were attributed to an electron-transfer rate associated with ionic-trapping effects, which were observed by electrochemical impedance spectroscopy. These results are discussed on the basis of dissipation and feedback effects.

Introduction

A great deal of attention has been given to WO_3 films, which may be used in several applications. For example, WO_3 films have been used in sensors to detect alcohol, acetone, and CS_2 gas molecules[1] and in photochromic devices, owing to the reversibility of the photochromic process upon exposure to oxygen.[2] Owing to its photoelectrochemical characteristics, nanoporous WO_3 can deliver high photocurrents, particularly in the oxidation of methanol and formic acid.[3] Electrodes formed from platinum, ruthenium, and WO_3 have shown enhanced electrocatalytic activity in comparison to the Pt−Ru alloy.[4] A thin layer of Pt deposited on a WO_3 film is a gaschromic material with coloring and bleaching processes under molecular hydrogen and oxygen atmospheres, respectively.[5] WO_3 is particularly relevant for electrochromic devices because of the changes in absorption—in the visible region—caused by the intervalence electron transfer from W(V) to W(VI) states.[6] Indeed, color changes from white to blue may be induced when WO_3 is reduced, and these changes vary with the number of ions (H^+, Li^+, K^+, etc.) inserted into the oxide matrix. Because these processes are reversible, WO_3 may be used in displays and smart windows.[7−9] The number of ions inserted may be controlled electrochemically through the following process:

$$WO_3 + xM^+ + xe^- \rightarrow M_xWO_3 \qquad (1)$$

Charge compensation requires that a cationic species be inserted (removed) when an electron is injected (removed) into (from) the conduction band.

The properties of WO_3 can be improved by the addition of TiO_2, as demonstrated in a number of cases. For example, a photoelectrochemical anticorrosion system comprising TiO_2 and WO_3 was developed to protect stainless steel.[10] WO_3 was used to store energy generated in a TiO_2 photocatalyst under UV radiation.[11] WO_3/TiO_2 films performed better than WO_3 in the photocatalytic decomposition of alcohols in the gas phase and may be used to decompose organic pollutants.[12] WO_3 colloids combined with TiO_2 nanoparticles displayed improved photochromic properties with more photogenerated electrons participating in the coloration

* Corresponding author e-mail: fritz@ffclrp.usp.br.
† Ciências e Letras de Ribeirão Preto.
‡ Instituto de Física de São Carlos.
§ Instituto de Química de São Carlos.

(1) Li, X.-L.; Lou, T.-J.; Sun, X.-M.; Li, Y.-D. *Inorg. Chem.* **2004**, *43*, 5443.
(2) Bechinger, C.; Oefinger, G.; Herminghaus, S.; Leiderer, P. *J. Appl. Phys.* **1993**, *74*, 4527.
(3) Santato, C.; Ulmann, M.; Augustynski, J. *J. Phys. Chem. B* **2001**, *105*, 936.
(4) Park, K.-W.; Choi, J.-H.; Ahn, K.-S.; Sung, Y.-E. *J. Phys. Chem. B* **2004**, *108*, 5989.
(5) Shanak, H.; Schmitt, H.; Nowoczin, J.; Ziebert, C. *Solid State Ionics* **2004**, *171*, 99.
(6) Faughnan, B. W.; Crandall, R. S.; Heyman, P. M. *RCA Rev.* **1975**, *36*, 177.
(7) Livage, J. *Solid State Ionics* **1992**, *50*, 307.
(8) Granqvist, C. G. *Sol. Energy Mater. Sol. Cells* **2000**, *60*, 201.
(9) Granqvist, C. G. *Electrochim. Acta* **1999**, *44*, 3005.
(10) Tatsuma, T.; Saitoh, S.; Ohko, Y.; Fujishima, A. *Chem. Mater.* **2001**, *13*, 2838.
(11) Tatsuma, T.; Saitoh, S.; Ngaotrakanwiwat, P.; Ohko, Y.; Fujishima, A. *Langmuir* **2002**, *18*, 7777.
(12) Song, K. Y.; Park, M. K.; Kwon, Y. T.; Lee, H. W.; Chung, W. J.; Lee, W. I. *Chem. Mater.* **2001**, *13*, 2349.

10.1021/cm051113q CCC: $30.25
Published on Web 11/24/2005

process.[13] Electrochromic materials based on WO_3 doped with TiO_2 may have increased reversibility of the insertion/deinsertion process, charge capacity, optical density, and lifetime.[14−16]

There are several techniques for the deposition of WO_3 and TiO_2 on glass. Amorphous WO_3 and TiO_2 films can be prepared by vacuum evaporation, sputtering, anodic oxidation, sol−gel synthesis, electron-beam, magnetron, and rf-sputtering.[8] Our interest lies in the production of layer-by-layer (LbL) films from WO_3 and TiO_2, to exploit the control of molecular architecture. Using the LbL method, judiciously chosen architectures of transition metal oxides and spacer polymer layers can lead to structures with the desired electrochemical and electrochromogenic properties. Recent works have indicated that LbL films are promising for the fabrication of electrochromic devices due to the film uniformity and the possibility of controlling the thickness and the nanoarchitecture.[17−20] Several works have been reported on LbL films of TiO_2 particles. For instance, LbL films from TiO_2 and poly(allylamine hydrochloride) (PAH), polyethylenimine, and polyaniline have been used in electronic systems.[21] LbL films of 11-aminoundecanoic acid capped TiO_2 and PAH exhibited a rectifying behavior, typical of a Schottky diode, when sandwiched between indium-tin-oxide (ITO) and Au electrodes.[22] TiO_2 nanoparticles were immobilized in a LbL film of PAH and poly(acrylic acid) (PAA), with their photocatalytic properties for the oxidation of iodide and the decomposition of methyl orange being preserved.[23] This LbL film was also obtained by the sequential deposition of PAH/PAA/TiO_2/PAA and tested as a gas sensor for ammonia and relative humidity.[24] Solar cells fabricated with polyion/TiO_2 LbL films exhibited efficiency comparable to that observed for materials obtained by conventional deposition methods.[25] A nanoporous LbL film of TiO_2 and phytic acid deposited on ITO was used to control the electrochemical properties of a hemoglobin-modified electrode.[26]

In contrast to the frequent use of TiO_2, only a few papers have described the incorporation of WO_3 in LbL films, and reference should be made to the work of Chen and co-workers.[27,28] In the latter work, the authors described the fabrication of superlattice thin films comprising WO_3 alternately assembled with either 4,4′-bis-5-pyridium-pentyloxybiphenyl (4,4′-BPPOBp) or 4,4′-bis(aminomethyl)-biphenyl (4,4′-BAMBp) dihydrochloride. The films displayed a well-ordered structure in the *z*-axis and had photochromic properties.

In this work, TiO_2 is immobilized in LbL films made with chitosan/WO_3. The choice of chitosan was based on its ability to form complexes with oxides in solutions,[29,30] thus serving as a good template material for the uniform growth of multilayers. Chitosan is the deacetylated form of chitin, a polysaccharide that can be extracted from the shells of crabs and the exoskeletons of shrimp and other arthropods.[31] This polymer is stable in the potential range commonly used, and it is colorless due to the small amount of material deposited with the LbL method. This means that chitosan does not hamper the electrochromic properties of the transition metal oxide. Besides, complexes formed with chitosan can ensure a high proton conductivity.[32] The effect of the addition of TiO_2 on the electrochromogenic properties is also studied. The quadratic logistic equation (QLE) is used to describe the absorbance change (ΔA), absorption coefficient (ϵ), and electrochromic efficiency (η) as a function of the charge injected.[33−37] Finally, electronic trapping is discussed on the basis of electrochemical impedance spectroscopy results and is associated with dissipation and feedback effects.

Experimental Details

WO_3 xerogel was synthesized following a sol−gel method described in the literature.[18,38] Briefly, a sodium tungstate (Na_2WO_4) solution 0.25 mol.L^{-1} was added to a proton-exchange resin, leading to a yellowish liquid of tungstic acid (H_2WO_4). This solution became turbid in ca. 2 h at 25 °C (pH = 1.5). The colloidal dispersion of TiO_2 was prepared by the hydrolysis of tetra-*n*-butyl titanate from DuPont (Tyzor). A mixture of 30 mL of the organic titanate and 30 mL of 2-propanol was slowly added (15 min) to 300 mL of deionized water under vigorous stirring. To this mixture was added 2 mL of a 70% nitric acid (while stirring). The resulting solution was stirred for 2 h at room temperature. The mixture was then heated to 80 °C while stirring for 4 h, giving rise to a stable and transparent (slightly cloudy) TiO_2

(13) He, T.; Ma, Y.; Cao, Y.; Hu, X.; Liu, H.; Zhang, G.; Yang, W.; Yao, J. *J. Phys. Chem. B* **2002**, *106*, 12670.
(14) Hashimoto, S.; Matsuoka, H. *J. Electrochem. Soc.* **1991**, *138*, 2403.
(15) Gottsche, J.; Hinsch, A.; Wittwer, V. *Sol. Energy Mater. Sol. Cells* **1993**, *31*, 415.
(16) Livage, J.; Guzman, G. *Solid State Ionics* **1996**, *84*, 205.
(17) Huguenin, F.; Ferreira, M.; Zucolotto, V.; Nart, F. C.; Torresi, R. M.; Oliveira, O. N. *Chem. Mater.* **2004,** *16*, 2293.
(18) Ferreira, M.; Huguenin, F.; Zucolotto, V.; da Silva, J. E. P.; de Torresi, S. I. C.; Temperini, M. L. A.; Torresi, R. M.; Oliveira, O. N., Jr. *J. Phys. Chem. B* **2003**, *107*, 8351.
(19) Huguenin, F.; dos Santos, D. S.; Bassi, A.; Nart, F. C.; Oliveira, O. N. *Adv. Funct. Mater.* **2004**, *14*, 985.
(20) DeLongchamp, D. M.; Hammond, P. T. *Chem. Mater.* **2004**, *16*, 4799.
(21) Kovtyukhova, N.; Ollivier, P. J.; Chizhik, S.; Dubravin, A.; Buzaneva, E.; Gorchinskiy, A.; Marchenko, A.; Smirnova, N. *Thin Solid Films* **1999**, *337*, 166.
(22) Cassagneau, T.; Fendler, J. H.; Mallouk, T. E. *Langmuir* **2000**, *16*, 241.
(23) Kim, T.-H.; Sohn, B.-H. *Appl. Surf. Sci.* **2002**, *201*, 109.
(24) Kim, J. H.; Kim, S. H.; Shiratori, S. *Sens. Actuators, B* **2004**, *102*, 241.
(25) He, J.-A.; Mosurkal, R.; Samuelson, L. A.; Li, L.; Kumar, J. *Langmuir* **2003**, *19*, 2169.
(26) Paddon, C. A.; Marken, F. *Electrochem. Commun.* **2004**, *6*, 1249.
(27) Chen, Z.-H.; Ma, Y.; Yao, J. N. *Thin Solid Films* **2001**, *384*, 160.
(28) Chen, Z.-H.; Yang, Y.-A.; Qiu, J.-B.; Yao, J.-N. *Langmuir* **2000**, *16*, 722.
(29) Guzmán, J.; Saucedo, I.; Navarro, R.; Revilla, J.; Guibal, E. *Langmuir* **2002**, *18*, 1567.
(30) Navarro, R.; Guzmán, J.; Saucedo, I.; Revilla, J.; Guibal, E. *Macromol. Biosci.* **2003**, *3*, 552.
(31) dos Santos, D. S.; Bassi, A.; Rodrigues, J. J.; Misoguti, L.; Oliveira, O. N.; Mendonça, C. R. *Biomacromolecules* **2003**, *4*, 1502.
(32) Smitha, B.; Sridhar, S.; Khan, A. A. *Macromolecules* **2004**, *37*, 2233.
(33) May, R. M. *Nature* **1976**, *261*, 459.
(34) Gonzalez, E. R. *J. Electrochem. Soc.* **1996**, *143*, L113.
(35) Torresi, R. M.; Cordoba de Torresi, S. I.; Gonzalez, E. R. *J. Electroanal. Chem.* **1999**, *461*, 161.
(36) Strogatz, S. H. *Non Linear Dynamics and Chaos*; Addison-Wesley Publishing Co.: Reading, MA, 1994; p 353.
(37) Huguenin, F.; Nart, F. C.; Gonzalez, E. R.; Oliveira, O. N. *J. Phys. Chem. B* **2004**, *108*, 18919.
(38) Chemseddine, A.; Henry, M.; Livage, J. *Rev. Chim. Miner.* **1984**, *21*, 487.

suspension (pH = 2). The effective diameter of the colloidal TiO_2 particles was 17.3 nm, as determined by dynamic light scattering (DLS) in a Brookhaven Instruments Corp. machine. The solution was cooled, displaying no change in its transparency, and remained stable for at least 6 months. Commercial chitosan from shrimp, with 1200 cPs viscosity (1 wt % solution in 2% v/v acetic acid solution) and deacetylation degree of 85%, was purchased from Galena Química Ltda, Brazil.

Layer-by-layer (LbL) films were assembled onto ITO-coated glass purchased from Flexitec (Curitiba, Brazil), with a sheet resistance $\leq 20\ \Omega$ and a geometrical area of 1 cm^2. The layers of the LbL chitosan/WO_3 film were obtained via ionic attraction of oppositely charged materials, by the alternated immersion for 3 min of the ITO substrate into the polycationic (chitosan 1.6 g L^{-1} and pH = 2) and then into the anionic (WO_3 0.25 mol L^{-1} and pH = 1.5) dispersions. This sequence was repeated four times. After deposition of each layer, the substrates were rinsed for 30 s in HCl solution (pH = 2) and dried under a nitrogen flow. The as-deposited (chitosan/WO_3)$_4$ films were characterized electrochemically prior to the deposition of the TiO_2 layer, which was carried out by the immersion of the (chitosan/WO_3)$_4$ films into a colloidal dispersion of TiO_2 for 1 min, followed by rinsing in HCl solution (pH = 2) and drying under a nitrogen flow. This procedure resulted in the formation of (chitosan/WO_3)$_4$/TiO_2 films. Another set of samples was prepared in the following sequence: chitosan/WO_3/chitosan/TiO_2, with a deposition time of 3 min in each step. This sequence was also repeated four times. After deposition of each composite layer, the substrates were rinsed and dried under the same conditions described above. This electrode is referred to as (chitosan/WO_3/chitosan/TiO_2)$_4$. Previous experiments showed a linear growth of the chitosan/WO_3 multilayers, in which the same amount of material was absorbed at each deposition step (results shown elsewhere[39]). The thickness of the films was measured with a Talystep profilometer.

Electrochemical experiments were carried out with an Autolab PGSTAT30 potentiostat/galvanostat. The counter electrode used was a platinum sheet with an area of 10 cm^2. The reference electrode was a saturated calomel electrode (SCE), and the electrolyte solution was HCl (pH = 2). Chromogenic analysis was made simultaneously with the electrochemical experiments using a microprocessor-controlled solid-state light source (WPI, Inc.). Plastic fiber optic cables up to 1 mm in diameter were used to deliver red light (660 nm) from the instrument to a PDA1 photodiode amplifier (WPI, Inc.).

Results and Discussion

The thickness of the (chitosan/WO_3)$_4$ and (chitosan/WO_3)$_4$/TiO_2 LbL films was 60 and 70 nm, respectively, with an uncertainty of 5%. Because of the non-homogeneity of the (chitosan/WO_3/chitosan/TiO_2)$_4$ film, its thickness could not be determined precisely. Because the experimental conditions employed for film fabrication were the same for all films, one may expect that the thickness of each individual layer, namely chitosan, WO_3, and TiO_2, would be the same, but a straightforward comparison of the electrochromic properties with the other systems is not possible. The data from the (chitosan/WO_3/chitosan/TiO_2)$_4$ films will nevertheless be discussed here to better understand the influence of the TiO_2 particles on the electrochemical properties of chitosan/WO_3 layers.

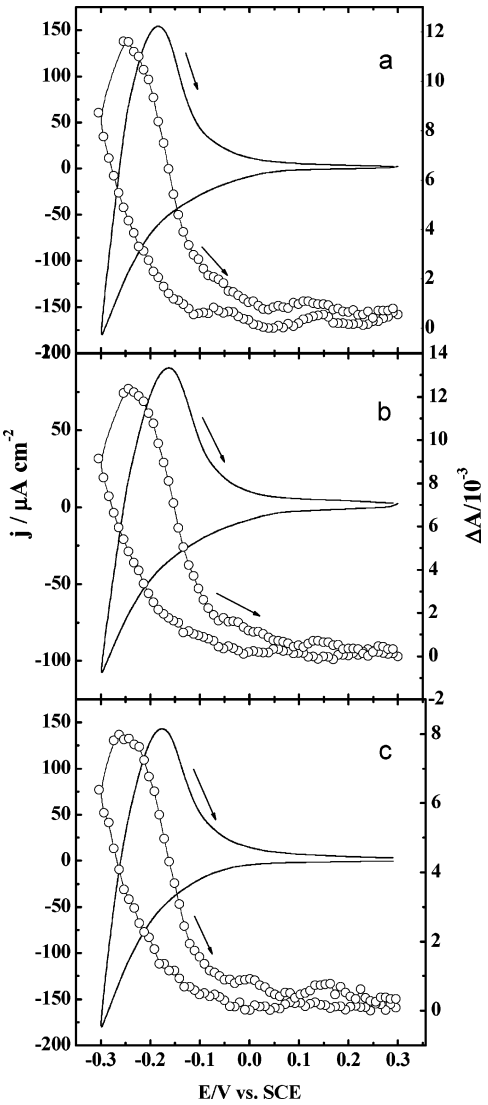

Figure 1. Profile of (—) current density, *j*, and (−○−) absorbance changes, Δ*A*, at 590 nm for 4-bilayer LbL films of (a) (chitosan/WO_3)$_4$, (b) (chitosan/WO_3)$_4$/TiO_2, and (c) (chitosan/WO_3/chitosan/TiO_2)$_4$ (ν = 50 mVs^{-1}).

The results for the layer-by-layer architectures introduced in this work, namely, (chitosan/WO_3)$_4$/TiO_2 and (chitosan/WO_3/chitosan/TiO_2)$_4$, will be discussed in connection with those obtained in an earlier work for the chitosan/WO_3 system.[39] Figure 1 shows the cyclic voltammograms for ITO electrodes covered with 4-bilayer LbL films of the systems above, which depict the proton insertion process during the negative potential scan and the proton deinsertion process during the positive potential scan at a rate of 50 mVs^{-1}. As the amount of WO_3 in the LbL films increases as a function of the number of bilayers,[39] the current density also increases when the number of bilayers increases from 1 to 4. The cyclic voltammograms in Figure 1 are similar, except for the magnitude of the current density, which shows that the extent

(39) Huguenin, F.; Gonzalez, E. R.; Oliveira, O. N. *J. Phys. Chem. B* **2005**, *109*, 12837.

of proton insertion/deinsertion is smaller in the (chitosan/WO_3)$_4$/TiO_2 film than in the other LbL films. This reduced insertion/deinsertion is attributed to the blocking effect of TiO_2 particles on the LbL film surface. A similar effect would be expected for the (chitosan/WO_3/chitosan/TiO_2)$_4$ film. However, the amount of material deposited in the latter film is larger in comparison to that for the (chitosan/WO_3)$_4$/TiO_2 film, as will be discussed below; thus, the observed current density is larger. In situ absorbance changes (ΔA) at 590 nm were measured simultaneously with the voltammograms. The absorbance changes are due to the electron transfer from W(V) to W(VI) sites, according to the electronic intervalence transfer model.[6] These systems are reversible, as demonstrated by the negligible value of ΔA after the voltammetric cycles, which also indicates that chitosan does not hinder the migration/diffusion of protons that compensate the charge injected.

Important information about the LbL systems can be obtained from the correlation of the absorbance change with the charge injected. In a previous work, we have shown that the quadratic logistic equation (QLE), expressed in eq 2, can be used for this purpose,[37]

$$\frac{dx}{dt} = sx\left(1 - \frac{x}{L}\right) \tag{2}$$

where x is the population of the electroactive species at the time t, dx/dt is the rate with which the population changes, and L and s are positive constants. At low values of x, $dx/dt \approx sx$, so s represents the normalized maximum rate of change and L is related to the system ability to sustain the population growth. For the system being studied here, the QLE describes the temporal evolution of the number of electrons ($N_{W(V)\rightarrow W(VI)}$) participating in the transfer from W(V) to W(VI) in the LbL films, analogous to what was reported for WO_3 in the absence of TiO_2.[39] The difference form of the QLE[33−37] can be written in this case as

$$\Delta A = rq\left(1 - \frac{q}{K}\right) \tag{3}$$

In this equation, K and r are constants, similar to L and s in eq 2. Moreover, the charge injected (q) is the population and ΔA takes the place of dq/dt. In fact, the magnitude of absorbance for WO_3 in the visible range depends on the charge (electron) transfer rate between W(V) and W(VI) sites and on the amount of charge injected. The constant K is associated with the system capability to sustain the growth of ($N_{W(V)\rightarrow W(VI),}$) and represents the maximum value of q. Thus, the number of electroactive oxide sites can be estimated by monitoring ΔA as a function of the charge injected (q).[37] For small values of q, $\Delta A \approx rq$ which shows that r is related to the electrochromic efficiency, as will be shown below. The method employed here, i.e., fitting the experimental data with the quadratic logistic equation (QLE), avoids the influence of the reduction of water. The term $(1 - q/K)$ represents the effects from dissipation and feedback, both contributing to the decrease of ΔA as q becomes large. As the number of electrons injected into the film increases, so does the number of protons, in accordance with eq 1. This increase of charge injected leads to the appearance of dissipative forces due to interactions among the protons and between the protons and the network. As the dissipative forces oppose charge transport (dq/dt) and increase with the amount of charge carriers (q), dissipation contributes to the feedback effect of ΔA (proportional to dq/dt) as a function of q. According to the site-saturation model,[40] another contribution to the feedback effect arises from the decrease in the number of sites available for the electronic intervalence transfer. This decrease occurs because an increase in the injected charge reduces the intervalence transfer W(V) → W(VI) flux.

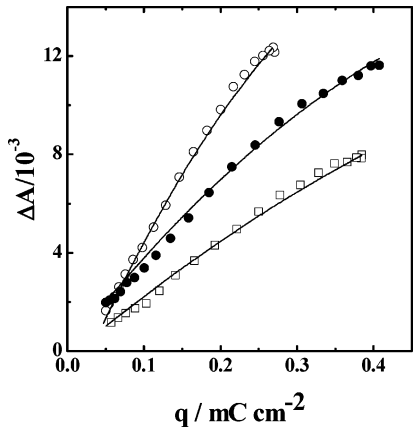

Figure 2. Plot of the theoretical (—) and experimental ΔA data at 590 nm as a function of charge for (−●−), (chitosan/WO_3)$_4$; (−○−), (chitosan/WO_3)$_4$/TiO_2; and (−□−), (chitosan/WO_3/chitosan/TiO_2)$_4$.

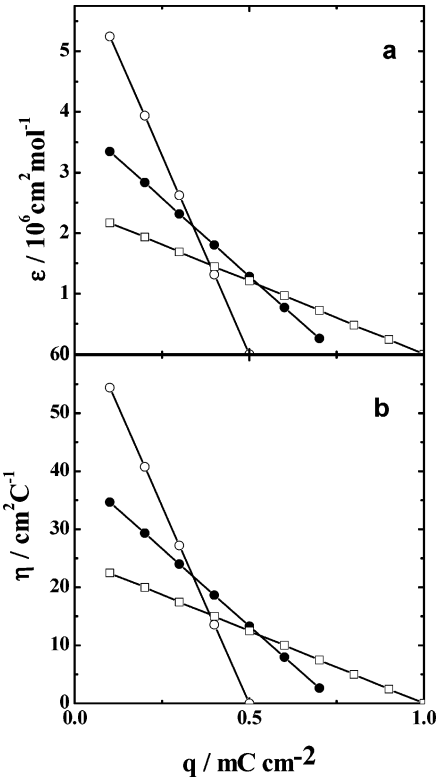

Figure 3. Plot of (a) the theoretical molar absorption coefficient and (b) the theoretical electrochromic efficiency at 590 nm as a function of charge for (−●−), (chitosan/WO_3)$_4$; (−○−), (chitosan/WO_3)$_4$/TiO_2; and (−□−), (chitosan/WO_3/chitosan/TiO_2)$_4$.

(40) Denesuk, M.; Uhlmann, D. R. *J. Electrochem. Soc.* **1996**, *143*, L186.

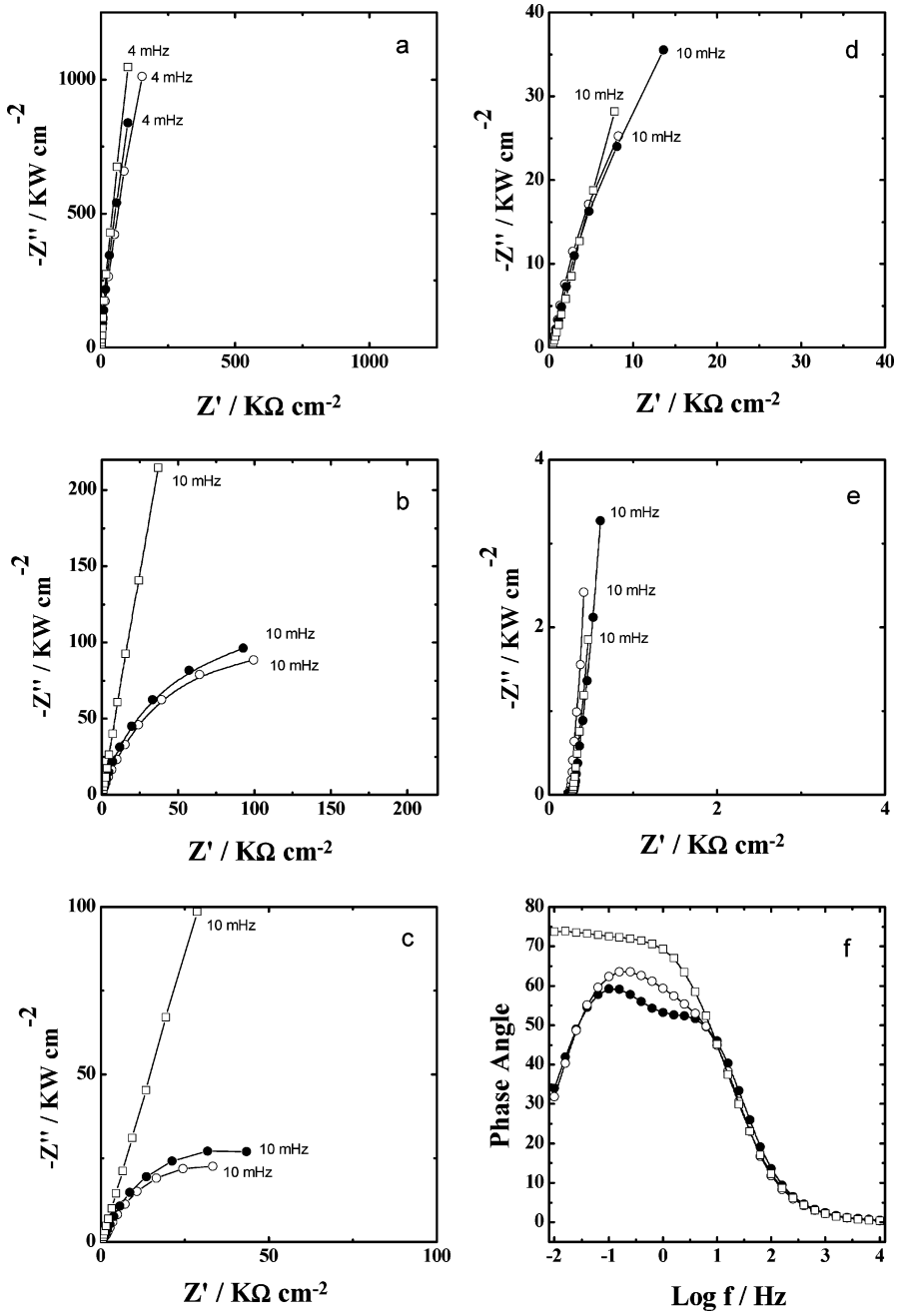

Figure 4. Nyquist diagrams obtained by applying a dc potential of (a) 0.3 V, (b) 0.1 V, (c) 0.0 V, (d) −0.1 V, and (e) −0.3 V for (−●−), (chitosan/WO_3)$_4$; (−○−), (chitosan/WO_3)$_4$/TiO_2; and (−□−), (chitosan/WO_3/chitosan/TiO_2)$_4$. (f) Phase angle as a function of log frequency for (−●−), (chitosan/WO_3)$_4$; (−○−), (chitosan/WO_3)$_4$/TiO_2; and (−□−), (chitosan/WO_3/chitosan/TiO_2)$_4$ LbL films.

Figure 2 shows ΔA curves as a function of the charge for the various systems investigated and includes the theoretical fittings with the QLE. The K and r values resulting from the fittings are 1.5 mCcm^{-2} and 40 cm^{2}C^{-1} for (chitosan/WO_3)$_4$, 1.0 mCcm^{-2} and 68 cm^{2}C^{-1} for (chitosan/WO_3)$_4$/TiO_2, and 2.0 mCcm^{-2} and 25 cm^{2}C^{-1} for (chitosan/WO_3/chitosan/TiO_2)$_4$, respectively. From these values, the number of electroactive W(V) sites was estimated as being ca. 15.5 $\times$ 10^{-9} mol cm^{-2}, 10.7 $\times$ 10^{-9} mol cm^{-2}, and 20.7 $\times$ 10^{-9} mol cm^{-2} for (chitosan/WO_3)$_4$, (chitosan/WO_3)$_4$/TiO_2, and (chitosan/WO_3/chitosan/TiO_2)$_4$, respectively. It is now possible to understand the lower current density in the CV of Figure 1 for (chitosan/WO_3)$_4$/TiO_2. When TiO_2 particles are deposited on the film surface, some WO_3 sites are blocked to the access of protons, thus decreasing the number of electroactive sites.

Assuming that the molar absorption coefficient (ϵ) and the electrochromic efficiency (η) can be related by[41]

$$\eta = \frac{\mathrm{d}(\Delta A)}{\mathrm{d}q} = \frac{\epsilon}{zF} \tag{4}$$

where z is the charge of this species and F is Faraday's constant. The QLE can be used to determine ϵ and η by substituting ΔA from eq 3. Thus,

$$\epsilon = zFr\left(1 - \frac{2q}{K}\right) \tag{5}$$

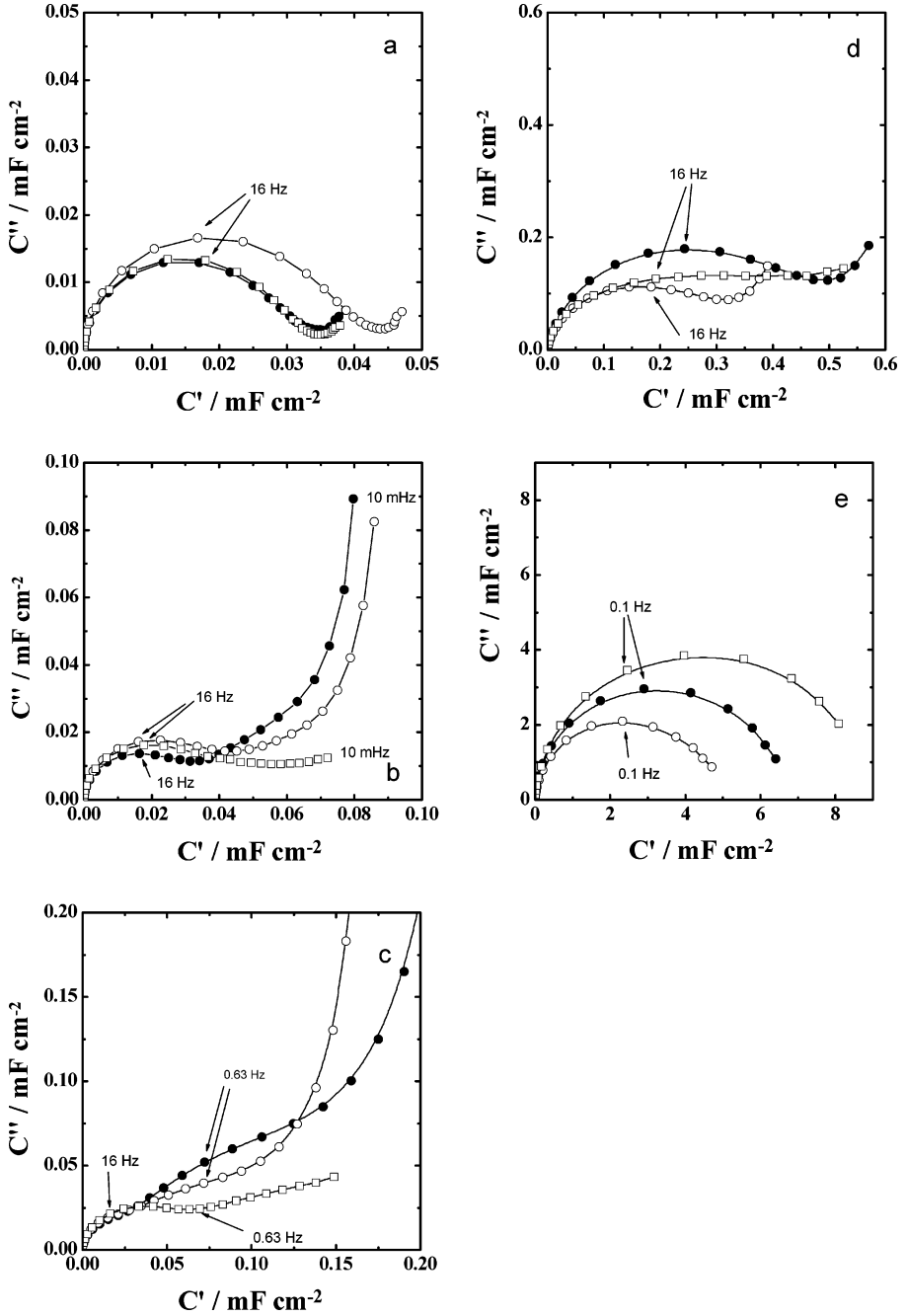

Figure 5. Complex plane representation of the capacitance obtained by applying a dc potential of (a) 0.3 V, (b) 0.1 V, (c) 0.0 V, (d) −0.1 V, and (e) −0.3 V for (−●−), (chitosan/WO_3)$_4$; (−○−), (chitosan/WO_3)$_4$/TiO_2; and (−□−), (chitosan/WO_3/chitosan/TiO_2)$_4$.

and

$$\eta = r\left(1 - \frac{2q}{K}\right) \tag{6}$$

Figure 3 shows the molar absorption coefficient and the electrochromic efficiency for the LbL films, obtained from eqs 5 and 6 for a charge between zero and a value at which ΔA is expected to be independent of q ($=K/2$). The values of ϵ and η for (chitosan/WO_3/chitosan/TiO_2)$_4$ are smaller than those for the other LbL films studied here due to the irregularity of the film, which can be observed by visual inspection. Nevertheless, ϵ and η decrease faster with q for (chitosan/WO_3)$_4$/TiO_2 because of the greater dissipation and feedback effects. The difference in the molar absorption coefficient and electrochromic efficiency for the LbL films will be discussed below, together with the impedance data.

In previous works,[42,43] impedance spectroscopy was used to distinguish between interfacial and bulk processes, as this technique allows one to examine mechanisms with different relaxation times. Figure 4 shows the Nyquist diagrams and the Bode plot of the phase angle, while Figure 5 shows the complex plane representation of the capacitance, in which the (chitosan/WO_3)$_4$, (chitosan/WO_3)$_4$/TiO_2, and (chitosan/WO_3/chitosan/TiO_2)$_4$ LbL films were subjected to dc poten-

(41) Maranhão, S. L. A.; Torresi, R. M. *Electrochim. Acta* **1998**, *43*, 257.
(42) Bueno, P. R.; Leite, E. R. *J. Phys. Chem. B* **2003**, *107*, 8868.
(43) Bisquert, J. *Electrochim. Acta* **2002**, *47*, 2435.

tials of 0.3, 0.1, 0.0, −0.1, and −0.3 V, with 5 mV of ac amplitude superimposed. The results in Figure 4a show semicircles associated with resistive and capacitive processes in parallel. These coupled processes are related to the interface and can be represented by the charge-transfer resistance (R_{ct}) and the double-layer capacitance (C_{dl}). However, bulk processes appear at low frequencies (<1 Hz) for more negative potentials and are due to proton diffusion and trapping—as already discussed in the literature for WO_3 and intercalation electrodes.[42,43] As in the previous work,[43] the LbL films are assumed to comprise regions separated by energy barriers of different heights, and therefore, protons take longer to overcome some of the barriers (trapping) than others (diffusion). Finite diffusion processes are observed more clearly at −0.3 V in Figure 4e, where the straight lines almost parallel to the imaginary axis at low frequencies represent finite diffusion. A semi-infinite diffusion process could not be observed because the samples are very thin (ca. 60−70 nm). These bulk processes can be observed at low frequencies in Figure 4f, which shows the phase angle as a function of frequency at 0.0 V for the LbL films. Interfacial and bulk processes are observed at $f > 1$ Hz and $f < 1$ Hz, respectively. The distinction between trapping and interfacial processes is better visualized in the complex plane representation of the capacitance, as shown in Figure 5. The width of the semicircle gives the capacitance value. The first semicircle—at high frequencies—is related to the $R_{ct}C_{dl}$ relaxation, and the second semicircle is associated with the R_tC_t couple (trap resistance and capacitance), which is more visible at 0.0 V. This trapping process occurs in parallel with the proton-diffusion process, for which the semicircles are shown in Figure 5e (at −0.3 V).

From these results, we conclude that the double-layer capacitance (C_{dl}) for (chitosan/WO_3)$_4$ (∼30 μCcm^{-2}) is slightly smaller than that of (chitosan/WO_3)$_4$/TiO_2 (∼40 μCcm^{-2}) at 0.3 V. Interestingly, at 0.3 V, the value of C_{dl} for (chitosan/WO_3)$_4$ is similar to that of (chitosan/WO_3/chitosan/TiO_2)$_4$. But the double-layer capacitance for (chitosan/WO_3/chitosan/TiO_2)$_4$ is slightly larger in comparison with (chitosan/WO_3)$_4$ at 0.1 V, which may be attributed to electrons trapped in surface states of TiO_2.[1] For this same potential, the semicircle associated with the bulk process indicates a greater capacitance for (chitosan/WO_3)$_4$ than for the other films. This is due to the proton trapping effect, which can be observed at 0.0 V. Particles of TiO_2 seem to decrease this trapping process. In fact, the (chitosan/WO_3/chitosan/TiO_2)$_4$ film, which contains TiO_2 in each bilayer of the LbL film, displayed the lowest capacitance. Acid TiO_2 sites interact with WO_3, and this may block the access of protons to the trapping sites. However, the presence of TiO_2 particles also decreases the access of protons to other WO_3 sites, as indicated by the finite diffusion capacitance for (chitosan/WO_3)$_4$/TiO_2 at −0.3 V (Figure 5e). The larger capacitance at −0.3 V for (chitosan/WO_3/chitosan/TiO_2)$_4$ is probably due to a larger amount of WO_3 than in the other films. This will be analyzed in future work.

The smaller trapping effect of (chitosan/WO_3)$_4$/TiO_2 is at least partially responsible for the higher value of r in eq 3. Since ionic trapping may decrease the electronic intervalence transfer W(V) → W(VI), the molar absorption coefficient and the electrochromic efficiency are decreased. The interactions between the ion and the network (trapping) are responsible for dissipation, which is associated with feedback effects, as expressed by the QLE.

Conclusions

The complexation capability of chitosan with transition metal oxides allowed the growth of LbL films of WO_3 and TiO_2, leading to visually uniform layer-by-layer films. Furthermore, the electrochemical properties associated with WO_3 were preserved because the presence of chitosan did not hamper the proton migration/diffusion into the LbL film. The deposition of a single TiO_2 layer deposited on top of the WO_3 layer in the (chitosan/WO_3)$_4$/TiO_2 resulted in more homogeneous films, which was advantageous for the electrochromic properties. As in previous works,[37,39] using QLE makes it possible to determine the number of electroactive sites, providing an estimate of the amount of WO_3 in the LbL films. Moreover, it was possible to use the QLE to estimate the absorption coefficient and electrochromic efficiency of the LbL films as a function of the charge injected. The interactions between the charge and the lattice are responsible for the dissipation and feedback effects and could also be analyzed. The LbL film formed from chitosan/WO_3 showed a higher molar absorption coefficient and electrochromic efficiency for small values of q when TiO_2 particles were deposited on the film surface. The addition of TiO_2 particles hindered the access of protons to the trapping sites, producing a lattice with low-height energy barriers, as observed with electrochemical impedance spectroscopy. Thus, electrons are more delocalized in the network, allowing a greater W(V) → W(VI) flux for small values of q, which promotes greater dissipation and feedback effects than in related LbL films without TiO_2.

Acknowledgment. Financial support from FAPESP, CNPq, and Capes (Brazil) is gratefully acknowledged.

CM051113Q